

Supporting Information for

Simultaneous Enhancement of Photoluminescence, MRI Relaxivity, and CT Contrast by Tuning the Interfacial Layer of Lanthanide Heteroepitaxial Nanoparticles

*Sha He,[†] Noah J. J. Johnson,[‡] Viet Anh Nguyen Huu,[†] Esther Cory,[§],[#] Yuran Huang,[□] Robert
L. Sah,^{§,□#} Jesse V. Jokerst,^{†,□*} and Adah Almutairi^{†,‡,□*}*

[†]Department of NanoEngineering, Jacobs School of Engineering, University of California, San Diego, 9500 Gilman Dr., La Jolla, United States

[‡]Skaggs School of Pharmacy and Pharmaceutical Sciences, University of California, San Diego, 9500 Gilman Dr., La Jolla, United States

[§] Department of Bioengineering, Jacobs School of Engineering, University of California, San Diego, 9500 Gilman Dr., La Jolla, United States

[□]Materials Science and Engineering Program, University of California, San Diego, 9500 Gilman Dr., La Jolla, United States

[#]Department of Orthopaedic Surgery, University of California, San Diego, 9500 Gilman Dr., La Jolla, United States

MATERIALS AND METHODS

Chemicals

Erbium acetate hydrate (99.9%), ytterbium acetate hydrate (99.9%), yttrium acetate hydrate (99.9%), gadolinium oxide (anhydrous, 99.9%), sodium trifluoroacetate (98%), trifluoroacetic acid, 1-octadecene (>90%), oleic acid (>90%), oleylamine (>70%), sodium hydroxide, methanol, chloroform, ethanol, and toluene were all purchased from Sigma. Ammonium fluoride was purchased from Spectrum. Lutetium oxide (anhydrous, 99.9%) was purchased from Alfa Aesar. 1,2-distearoyl-sn-glycero-3-phosphoethanolamine-N-[(polyethylene glycol)-2000] (DSPE-PEG-2000) was purchased from Avanti Lipids. Gadolinium (III) 1, 4, 7, 10-tetraazacyclododecane-1,4,7,10-tetraacetate (Gd-DOTA) was purchased from Macrocyclics. Hexabrix (sodium and meglumine ioxaglate) was purchased from Guerbet. All chemicals were used as received without further purification unless specified.

We synthesized the hexagonal phase (β)- $\text{NaYb}_{0.2}/\text{Er}_{0.8}\text{F}_4@/\text{NaLuF}_4@/\text{NaGdF}_4$ hetero-epitaxial core-shell-shell (CSS) nanoparticles (NPs) by following our previously published procedure.¹ In this procedure, cubic phase (α)- NaLuF_4 (Figure S1) and NaGdF_4 (Figure S2) NPs were synthesized separately, cleaned, and injected into the β - NaYb/ErF_4 core NPs reaction mixture at high temperature to obtain CSS structures (Figure S3).

Synthesis of cubic (α)- NaLuF_4 NPs (Sacrificial shell NPs)

Cubic NaLuF_4 were synthesized according to our previously reported procedure.¹ Briefly, Lu_2O_3

(1 mmol) was dissolved in 50% aqueous trifluoroacetic acid (20 mL), refluxed overnight at 95 °C, and dried overnight at 70 °C remaining ~2 mmol lutetium trifluoroacetate as white powder. Sodium trifluoroacetate (2 mmol), 1-octadecene (12 mL), oleic acid (6 mL), and oleylamine (6 mL) was added to the prepared lutetium trifluoroacetate with vigorous stirring. The obtained yellow slurry was quickly heated to 120 °C under mild vacuum and maintained for 30 min to yield a clear yellow solution. The clear solution was switched under a gentle argon flow, heated to 300 °C rapidly (~15°C/min), and maintained at 300 °C with vigorous stirring until the solution became cloudy. The cloudy solution was kept 300 °C for ~12 min to obtain kinetically-stable α -NaLuF₄ NPs with an average size of ~8.27 nm (Figure S1). The synthesized NPs were naturally cooled to room temperature, precipitated by adding ethanol, collected by centrifugation (1900 g, 5 min), and washed with ethanol for several times. The final pellet was then dispersed in hexane (10 mL) as clear and colorless solution, and stored at 37 °C for further use.

Synthesis of cubic (α)-NaGdF₄ NPs (Sacrificial shell NPs)

Cubic (α)-NaGdF₄ were synthesized with the same protocol described above except that Gd₂O₃ (1.0 mmol) was used. The final product were kinetically-stable α -NaGdF₄ NPs with a size of ~6.18 nm (Figure S2) dispersed in hexane (10 mL).

Synthesis of hexagonal (β)-NaYb_{0.2}/Er_{0.8}F₄ core NPs

β -NaYb_{0.2}/Er_{0.8}F₄ core NPs were synthesized following our previous protocol with slight modification.¹ Briefly, 0.8 mmol of erbium acetate hydrate, 0.2 mmol ytterbium acetate hydrate,

1-octadecene (15 mL), and oleic acid (4.5 mL) were mixed, quickly heated to 120 °C under mild vacuum, kept at 120 °C for 45 min, and naturally cooled down to room temperature to yield a pinkish orange solution. A methanol solution (10mL) of ammonium fluoride (4 mmol) and sodium hydroxide (2.5 mmol) was added into the pinkish orange solution to yield a cloudy mixture. The mixture was stirred for 45 min at room temperature and slowly heated (~ 30 min) to 70 °C to remove methanol. The cloudy mixture became progressively clear during the heating process. Afterwards, it was quickly heated to 300 °C (~ 15 °C/min) and maintained at 300 °C for 1 h. Finally, the reaction mixture was cooled down and the NPs were precipitated by adding ethanol, collected by centrifugation (1900 g, 5 min), and washed several times with ethanol. The resulting pellet was then dispersed in chloroform (5 mL) for further studies.

Synthesis of hexagonal (β)-NaYF₄:Yb(18%)/Er(2%) NPs

β -NaYF₄:Yb(18%)/Er(2%) NPs were synthesized using a similar setup except that 0.8 mmol yttrium acetate hydrate, 0.18 mmol of ytterbium acetate hydrate, 0.02 mmol ytterbium, and 6 mL oleic acid were used.

Synthesis of hexagonal (β)-Na Yb_{0.2}/Er_{0.8}F₄@NaLuF₄@NaGdF₄ Hetero-epitaxial NPs

As synthesized sacrificial α -NaLuF₄ NPs (~ 1 mmol, see characterization section for details about quantification) in hexane were mixed with 1 mL 1-octadecene, gently stirred, and placed under a gentle flow of argon to remove hexane leaving NPs dispersed in 1-octadecene. After the β -NaYb/ErF₄ core NPs have been heated at 300 °C for 1 h, 1-octadecene dispersion of sacrificial

α -NaLuF₄ NPs was rapidly injected into the solution and allowed to ripen (12-15 min) to yield β -NaYb/ErF₄@NaLuF₄ core-shell (CS) NPs. To generate the thick shell in this study (9.7 nm thick NaLuF₄ shell on NaYb/ErF₄ core with diameter of 17.2 nm), repeated ($\times 9$) injections and ripening cycles (~ 9.4 mmol α -NaLuF₄ in total, see Table S4 for calculation) were performed while carefully maintaining the reaction mixture at 300 °C. After that, 0.96 mmol α -NaGdF₄ NPs were subsequently injected into the solution to yield hetero-epitaxial β -NaYb/ErF₄@NaLuF₄@NaGdF₄ CSS NPs. Finally, the reaction mixture was naturally cooled to room temperature. The CSS NPs were likewise precipitated by adding ethanol, collected by centrifugation (1900 g, 5 min), and washed with ethanol for several times. The resulting pellet was then dispersed in chloroform (5 mL) for further studies.

Synthesis of hexagonal (β)-NaYb/ErF₄@NaLuF₄@NaGdF₄ NPs with tunable thickness in the interfacial NaLuF₄ layer

The procedure was the same with the one above except that different amount of α -NaLuF₄ NPs were injected into the 1 mmol β -NaYb/ErF₄ core NPs solution at high temperature to obtain β -NaYb/ErF₄@NaLuF₄@NaGdF₄ CSS NPs with increasing thickness of interfacial NaLuF₄ layers. The amount of sacrificial α -NaLuF₄ and α -NaGdF₄ NPs used in the synthesis of each sample (Yb/ErG@Lu1@Gd, Yb/ErG@Lu2@Gd, and Yb/ErG@Lu3@Gd) were listed in Table S7.

Synthesis of hexagonal (β)-NaErF₄@NaGdF₄ CS NPs

The procedure was the same with that used for the Yb/Er@Lu@Gd CSS NPs except that 9 mmol of α -NaGdF₄ NPs were injected and ripened on the β -NaYb/ErF₄ core NPs without the use of α -NaLuF₄ NPs.

Characterization

The size and uniformity of the NPs were confirmed using transmission electron microscopy (TEM) (FEI, Technai G2 Sphera, operating at 120 kV). One droplet of the NP stock solution was diluted in 1 mL of hexane, drop cast onto a Pelco[®] carbon-coated 400 square mesh copper grid (Ted Pella, Inc.), and air dried for 1 hour before imaging. Scanning electron microscopy (SEM) images were obtained on FEI SFEG UHR SEM. The size distribution of the NPs was extracted from a representative TEM image by measuring at least 100 NPs, and presented as average \pm standard deviation. The energy-dispersive X-ray spectroscopy (EDS) was performed with a Tecnai G2 X-Twin (FEI Co.) instrument operating at 200 kV. Peaks in the EDS spectra were identified by comparison to a library of peaks *via* FEI software. The phase of NPs was determined by powder X-ray diffraction (XRD) using Siemens KFL Cu 2K diffractometer with a resolution of 0.02° and a scanning speed of 1°/min. The peaks in the XRD was reference to JCPDS file # 27-0689. Dynamic light scattering (DLS) measurements were performed using a Zetasizer Nano ZS (Malvern Instruments). Elemental concentration of all samples was determined by digesting the NPs in 70% HNO₃ for at least two days and analyzing on a Perkin Elmer Optima 3000 DV inductively coupled plasma atomic emission spectrometer (ICP-AES). All the photographs were taken with a Nikon[®] D5100 digital camera equipped with an AF-S

nikkor 18-55 mm, 1:3.5G-5.6G lens.

Morphological Characterization

The morphological characterization was performed following a previously published protocol.² Briefly, a representative TEM image of the each sample was converted to 8-bit binary image through the automatic threshold in ImageJ and outlined. Feret diameters, perimeters, and areas of NPs were measured automatically using the “analyzed particles” function in ImageJ. The circularity and roundness for all NPs were calculated by ImageJ, *via* the following equations:

$$\text{Roundness} = 4\text{Area}/[\pi(\text{Feret diameter})^2]$$

$$\text{Circularity} = 4\pi \text{Area}/(\text{Perimeter})^2$$

Where the Feret diameter is the major axis of the fitted ellipse that encloses one NP and the perimeter is the length of fitted ellipse around one NP. Since all analyzed samples were larger than 15 nm in diameters, we only collected the outlined NPs with areas larger than 176 nm^2 ($7.5^2 \times 3.14$) to eliminate errors.

Photoluminescence Spectra

Photoluminescent (including both upconversion and downconversion) emission spectra of different samples were collected with a FluoroLog modular spectrofluorometer (Horiba). The samples were excited by either an 808 nm (L808P1WJ, Thorlabs) or 980 nm (L9800P200, Thorlabs) continuous wave laser diode mounted on a temperature controlled laser diode mount (TCLDM9, Thorlabs). Emission in the visible range (400-700 nm) was recorded by the R928

PMT on FluoroLog while the emission in the NIR range (700-1200 nm) was recorded by the R5509 PMT. The R5509 PMT was cooled with excess liquid nitrogen for at least two hours before spectra recording. The integration time was set as 0.5 s. Emission was collected perpendicular to the direction of excitation light. 200 μ L chloroform solution of as-synthesized NPs was diluted with toluene (2 mL) to obtain a clear dispersion in a quartz cuvette (path length 1 cm) aiming for relatively low particle concentration suitable for optical measurements. Excitation power density was changed by tuning the controller while maintaining the beam cross-section unchanged. All spectra were corrected with the wavelength-dependent detector sensitivity provided by Horiba. Emission intensity was calculated by integrating the area under the curve using Origin Lab. The dark counts were subtracted from the integrated emission intensity before determining the enhancement factor.

Phase transfer of NP into water

For the CSS-NPs with diameter of 37.8 nm, 5 mg CSS-NPs (mass of one NP: $\sim 1.69 \times 10^{-13}$ mg, number of NPs in 5 mg: $\sim 3 \times 10^{13}$, ~ 0.05 nmol) in chloroform was mixed with 20 mg DSPE-PEG 2000 ($\sim 7 \times 10^3$ nmol) in a 20 mL screw-neck glass vial. The high molar ratio of DSPE-PEG 2000 to CSS-NPs ($\sim 10^5$) is critical to achieve high MRI relaxivity^{3,4} and it was kept for phase transfer of all other NPs in this study.

The vial containing the NPs and DSPE-PEG 2000 was left open overnight in a fume hood at room temperature to slowly evaporate chloroform leaving an oily layer at the bottom. The vial was mounted back to a rotary evaporator (Buchi R-205) at 60 °C for 1 h to completely remove

excess chloroform. Distilled water (10 mL) was slowly added into the vial and the NPs were transferred to water by sonicating the vial for 5 min (PEGylated NPs). The aqueous solution containing the PEGylated NPs was filtered twice through the 0.22 μm sterile polyethersulfone syringe filters (30 mm diameter, Low Hold-up volume, Olympus Plastics) and the PEGylated NPs were collected by using ultracentrifuge (Optima L-80 XP, Beckman Coulter) with the speed of 45000 rpm ($\sim 184,000g$) at 4 $^{\circ}\text{C}$ for 1 h. The supernatant with excess empty micelles composed of DSPE-PEG 2000 was carefully removed, and the pellet was re-dispersed into 5 mL distilled water and stored at 4 $^{\circ}\text{C}$ for further studies. When a higher concentration of the NPs was needed, the as-prepared aqueous solution was concentrated by centrifuge (3000g, 30 min) through a Vivaspin® 20 Centrifugal Concentrator (100K MWCO, PES) at the Allegra® X-15R Benchtop centrifuge (with a swing-out bucket).

Preparation of the aqueous DOTA solution

DOTA solution was prepared by dissolving 6.527 mg Gd-DOTA into 10 mL DI water to obtain a stock solution of 1 mM and diluted to designated concentrations accordingly before measurement.

MRI Relaxivity measurement at 1.41 Tesla

Longitudinal (T_1) relaxation times of all samples were measured at a Benchtop Bruker Minispec mq-60 relaxometer (60 MHz, 1.41 T at 37 $^{\circ}\text{C}$). Aqueous dispersion all samples were quantified by ICP-AES and tuned to 0.1 mM Gd^{3+} ionic concentration as the stock solution. The stock

solution was diluted to different concentrations (0.05 mM and 0.025 mM) and 200 μL of each sample was loaded into an NMR tube and measured respectively. For each measurement, application parameters for the relaxometer were: First pulse separation = 10 ms, final pulse separation = 10,000 ms, number of data points = 10, Delay sampling window = 0.05 ms, sampling window = 0.02 ms, time for saturation curve display = 3 s. r_1 MRI relaxivity was calculated by plotting $1/T_1$ against the ionic concentration of Ln^{3+} , fitting the scatter plot, and finding the slope of the fitting.

MRI Phantom studies at 7.0 Tesla

MR phantom images were obtained on a Bruker 7.0 T magnet equipped with Advance II Hardware and a 72 mm quadrature transmit/receive coil. All NPs and DOTA solution (200 μL) were loaded into the the 250 μL tubes and the tubes were immobilized into the agarose gel (1% wt) slab (6.5 cm \times 2 cm). The gel slab was scanned in the coil to obtain the cross-section images of all tubes simultaneously. T_1 relaxation time values at 7 T were determined by selecting regions of interest (ROI) using the ParaVision Version 5.1 software, and the fitting parameters were TR = 250.0 ms, TE = 12.6 ms, echo = 1/1, FOV = 6.91 cm/3.12 cm, slice thickness = 2.0 mm/3.0 mm, MTX = 256/116, FA = 180 deg. r_1 MRI relaxivity was also calculated by plotting $1/T_1$ against the ionic concentration of Ln^{3+} , fitting and scatter plot and finding the slope of the fitting.

Computed Tomography

CT contrast was determined on Micro-computed tomography scanner, Skyscan 1076 (Kontich, Belgium). Various aqueous samples in 250 μL tubes (including one tube filled with DI water as control group) were immobilized on a styrofoam stage inside the scanner and exposed to X-rays. Imaging was done at 36 μm isotropic voxel size, applying an electrical potential of 50 kVp and current of 200 μA , and using a 0.5 mm aluminum filter. A beam hardening correction algorithm was applied during image reconstruction. The obtained image intensity of water was set as 0 Hounsfield unit (HU) and air was set as -1000 HU to perform correlation between image intensity and HU values of various samples. Hexabrix (Guerbet, IN) was used as commercial contrast agent for comparison. A 2D orthogonal view of the full tube array was obtained using Dataviewer (Skyscan). The mean attenuation value of each sample was obtained on the cylindrical portion of the tube (5.33 mm height) and using a 3.88 diameter region of interest (ROI) which only covered the solution region and avoided the inner edge of the tube. The analysis was performed using CTAn software (Skyscan).

Surface area of the NPs

Surface area of the NPs (S) was calculated by the following equation

$$S = 4\pi r^2$$

Where r is the average radius of the NPs measured from the TEM images.

For $\alpha\text{-NaGdF}_4$ NPs, $r = 3.1$ nm, therefore $S = 0.12 \mu\text{m}^2$;

For $\beta\text{-NaYb/ErF}_4@NaLuF_4@NaGdF_4$ NPs, $r = 18.9$ nm, therefore $S = 4.5 \mu\text{m}^2$.

The surfaces of both $\alpha\text{-NaGdF}_4$ NPs and $\beta\text{-NaYb/ErF}_4@NaLuF_4@NaGdF_4$ NPs were

completely cover by NaGdF₄.

Tumbling time of the NPs (τ_R)

Tumbling time of the NPs (τ_R) was calculated by the following equation

$$\tau_R = 4\pi\eta a^3/3k_B T$$

Where η dynamic viscosity = 10^{-3} pa•s, $k_B T = 4 \times 10^{-21}$ J, a is the hydrodynamic radius of the NPs determined by DLS, T = 298 K.

Hydrodynamic radius of the α -NaGdF₄ NP is 6.5 nm (Figure S14), therefore the $\tau_R = 0.28$ μ s;

Hydrodynamic radius of the β -NaYb/ErF₄@NaLuF₄@NaGdF₄ NP is 23 nm (Figure S14), therefore the $\tau_R = 12.7$ μ s.


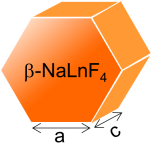
		Gadolinium (Gd)	Erbium (Er)	Ytterbium (Yb)	Lutetium (Lu)
	Ionic Radii (Å) ^{***}	1.193	1.144	1.125	1.117
	Unit Cell Volume (Å ³)	113.0	108.1	105.7	104.1
	Unit Cell Parameter a (Å)	6.020	5.959	5.929	5.901
	Unit Cell Parameter c (Å)	3.601	3.514	3.471	3.453

Table S1 Ionic properties of all four Ln³⁺ ions incorporated in the CSS NPs in this study. The ionic radius of lutetium is smaller than that of either erbium or ytterbium, allowing Frank–van der Merwe growth mode of NaLuF₄ shell on NaYb/ErF₄ core towards thick yet highly uniform epitaxial NaLuF₄ shells on NaYb/ErF₄ cores. The ionic radius of gadolinium is larger than that of lutetium allowing Stranski–Krastanov growth mode for a uniform thin NaGdF₄ shell on NaLuF₄.⁵

***Ionic radii of Ln³⁺ are for VIII coordinate species,⁶ and the β-NaLuF₄ unit cell parameters are from Joint Committee on Powder Diffraction Standards-International Centre for Diffraction Data (JCPDS-ICDD) database.

Samples	Designed radius (nm)	Designed layer thickness (nm)	Molar equivalency (mmol)
Yb/Er Core	8.6	8.6	1.0
Yb/Er@Lu CS	18.6	10.0	9.4
Yb/Er@Lu@Gd CSS	19.2	0.6	0.96

Table S2 Calculated molar equivalency of each Ln³⁺ for the synthesis of Yb/Er core, Yb/Er@Lu CS, and Yb/Er@Lu@Gd CSS NPs. On the synthesized Yb/Er core NPs with radii of 8.6 nm, we designed to achieve 10 nm thick NaLuF₄ shell and 0.6 nm NaGdF₄ shell on the cores. NaLuF₄ shell as thick as 10 nm effectively protects the excitation energy from surface quenching and concentration quenching at high doping level of Yb³⁺ and Er³⁺ in the core. NaGdF₄ shell as thin as 0.6 nm exposes all Gd³⁺ ions to the NP surfaces and maximizes the MRI relaxivity. To achieve this, 9.4 mmol of α -NaLuF₄ and 0.96 mmol α -NaGdF₄ sacrificial NPs need to be ripened and grown on the cores.

	Measured radius from TEM images (nm)	Compositions	Calculated molar equivalency (mmol)
Yb/Er Core	8.6	Yb + Er	1.0
Yb/Er@Lu CS	18.3	Lu	9.0
Yb/Er@Lu@Gd CSS	18.9	Gd	0.93

Table S3 Calculated molar equivalency of compositions in the Yb/Er@Lu@Gd CSS NPs by measuring the size of each sample on a representative TEM image. The molar ratio for (Yb+Er) / Lu / Gd is 1 / 9 / 0.93 and is consistent with the calculated amount in Table S2. We obtained 9 mmol out of the injected 9.4 mmol Lu and 0.93 mmol out of the injected 0.96 mmol Gd because of the minimal loss in the ripening process.

	Er ³⁺ (mM)	Yb ³⁺ (mM)	Lu ³⁺ (mM)	Gd ³⁺ (mM)
Yb/Er Core	2.41 ± 0.1	0.62 ± 0.1	/	/
Molar equivalency	(Er ³⁺ + Yb ³⁺) / Lu ³⁺ / Gd ³⁺ = 0.98 / 0 / 0			
Yb/Er@Lu CS	1.47 ± 0.1	0.38 ± 0.1	16.45 ± 0.3	/
Molar equivalency	(Er ³⁺ + Yb ³⁺) / Lu ³⁺ / Gd ³⁺ = 1 / 8.89 / 0			
Yb/Er@Lu@Gd CSS	2.07 ± 0.1	0.54 ± 0.1	23.29 ± 0.4	2.31 ± 0.1
Molar equivalency	(Er ³⁺ + Yb ³⁺) / Lu ³⁺ / Gd ³⁺ = 1 / 8.92 / 0.89			

Table S4 Elemental concentrations of different Ln³⁺ in core, CS, and CSS NPs obtained from ICP-AES, which is consistent with both Table S2 and Table S3.

	Characteristic absorption/emission wavelengths (nm)
Yb ³⁺	980
Er ³⁺	520, 540, 654, 808, 980, 1550
Lu ³⁺	/
Gd ³⁺	312

Table S5 Characteristic PL absorption/emission wavelengths for the Ln³⁺ used in this study.

	Gadolinium (Gd)	Erbium (Er)	Ytterbium (Yb)	Lutetium (Lu)
<i>4f</i> orbital	Half Filled	Partially Filled	Partially Filled	Filled
Unpaired electrons	7	3	1	0
Environment of the Unpaired Electrons	Isotropic	Anisotropic	Anisotropic	/
Electron Spin Relaxation Time (s)	10 ⁻⁸	10 ⁻¹³	10 ⁻¹³	10 ⁻¹³

Table S6 Paramagnetic properties of all four Ln³⁺ ions incorporated in the CSS NPs in this study.⁷

	Amount of core NPs (mmol)	Injected amount of the sacrificial NPs (mmol)	
	β -NaYb/ErF ₄	α -NaLuF ₄	α -NaGdF ₄
Yb/Er@Lu1@Gd	1.0	0.45	0.3
Yb/Er@Lu2@Gd	1.0	3.0	0.6
Yb/Er@Lu3@Gd	1.0	10	1.0

Table S7 The amount of sacrificial α -NaLuF₄ and α -NaGdF₄ NPs used to synthesize β -Yb/Er@Lu@Gd CSS NPs with increasing thickness of interfacial NaLuF₄ layers. The amount of the Yb/Er core NPs was kept at 1 mmol. The amount of α -NaGdF₄ NPs were calculated accordingly to ensure that the thickness of the outmost NaGdF₄ layer in the β -NaYb/ErF₄@NaLuF₄@NaGdF₄ CSS NPs remained as 0.6 nm.

	Radius	Measured Thickness (nm) of		Molar Equivalency (mmol)		
	(nm)	NaLuF ₄ Layer	NaGdF ₄ Layer	Er	Lu	Gd
Yb/Er@Lu1@Gd	10.2	1.0	0.6	1.0	0.41	0.27
Yb/Er@Lu2@Gd	14.1	4.9	0.6	1.0	2.96	0.52
Yb/Er@Lu3@Gd	19.3	10.1	0.6	1.0	9.61	0.97

Table S8 molar equivalency of each component in the β -NaYb/ErF₄@NaLuF₄@NaGdF₄ CSS NPs with tunable interfacial NaLuF₄ layers. The obtained molar equivalency is consistent with that in the Table S7.

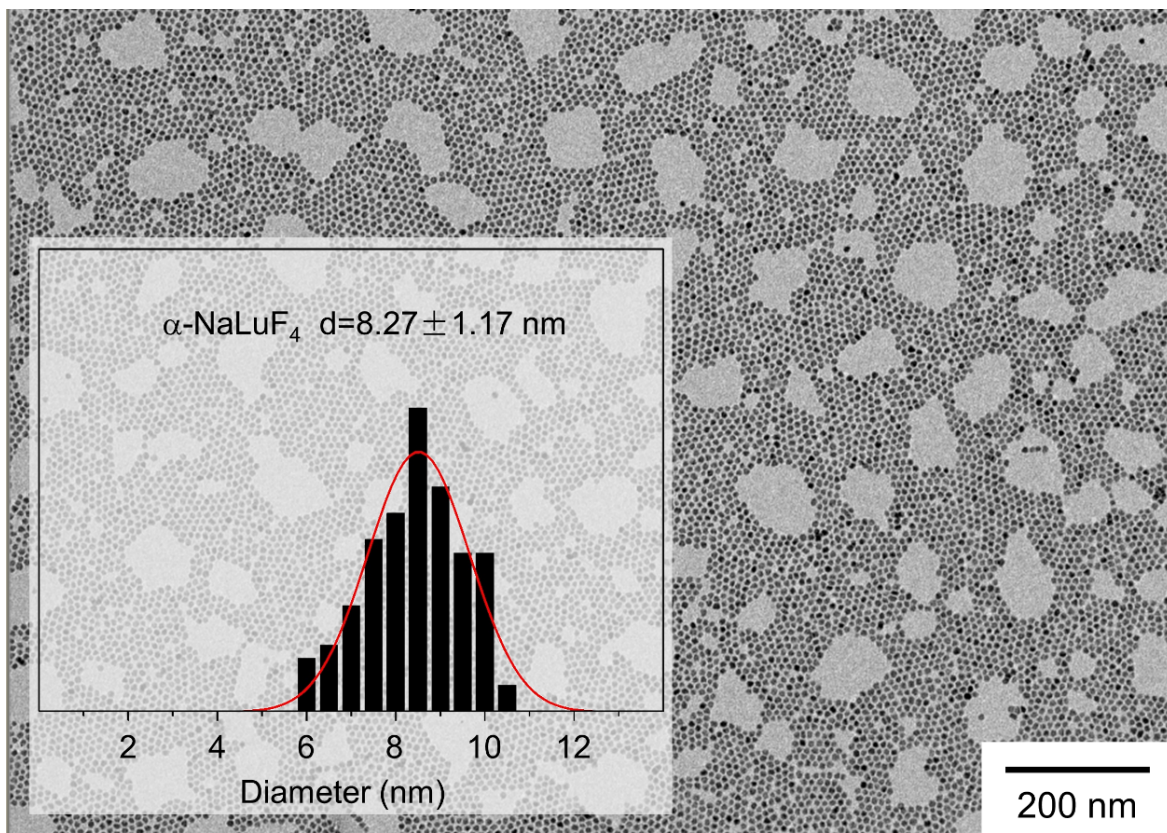


Figure S1 TEM image and size distribution of the α -NaLuF₄ NPs.

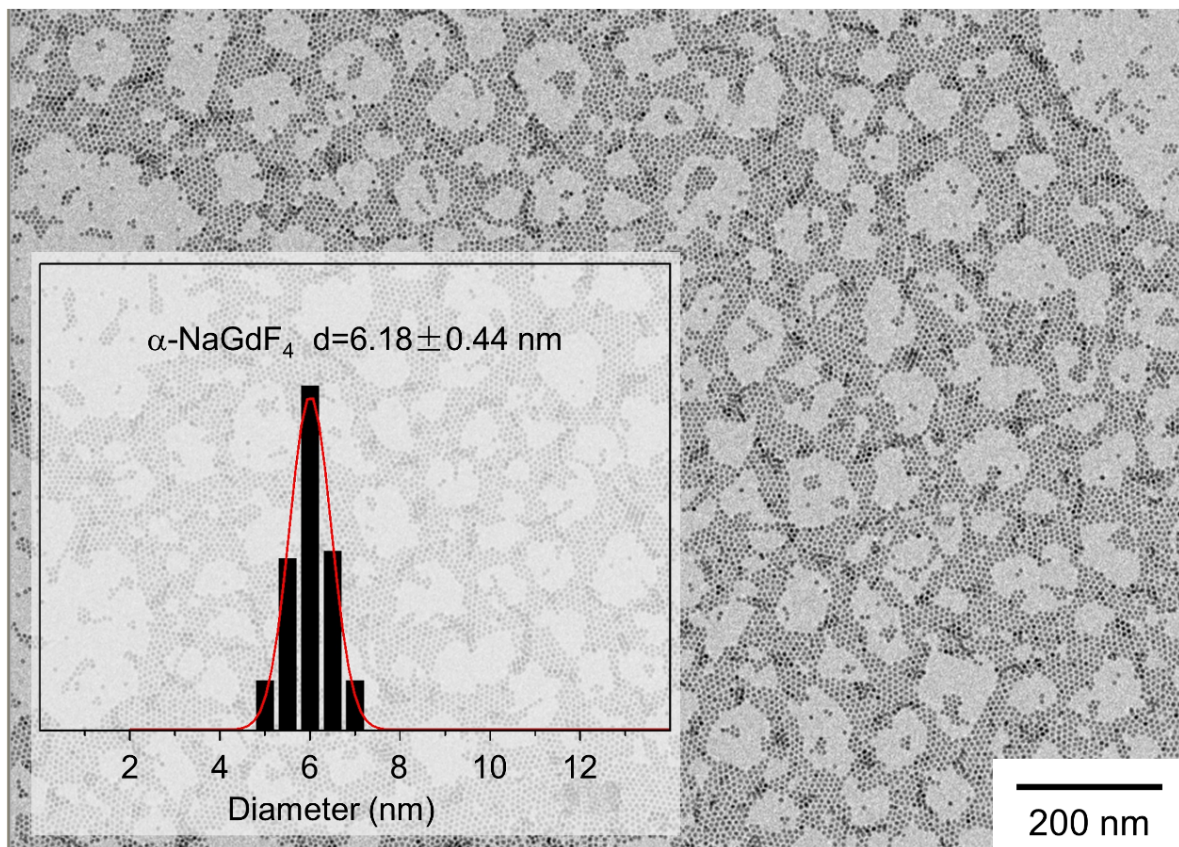


Figure S2 TEM image and size distribution of the α -NaGdF₄ NPs.

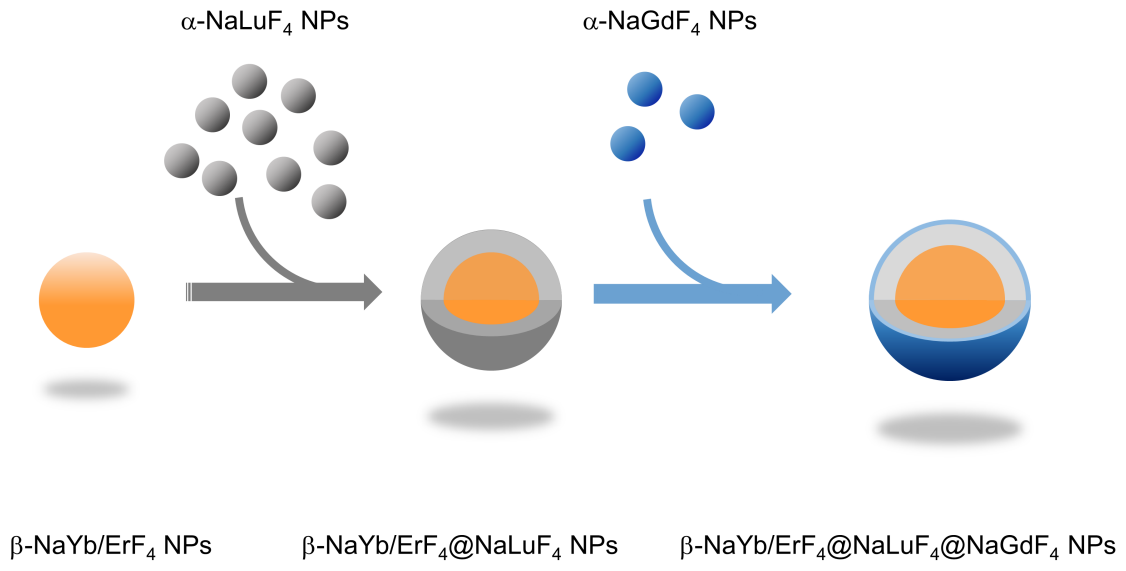


Figure S3 Schematic illustration for the synthesis procedure for $\beta\text{-NaYb/ErF}_4\text{@NaLuF}_4\text{@NaGdF}_4$ CSS NPs.

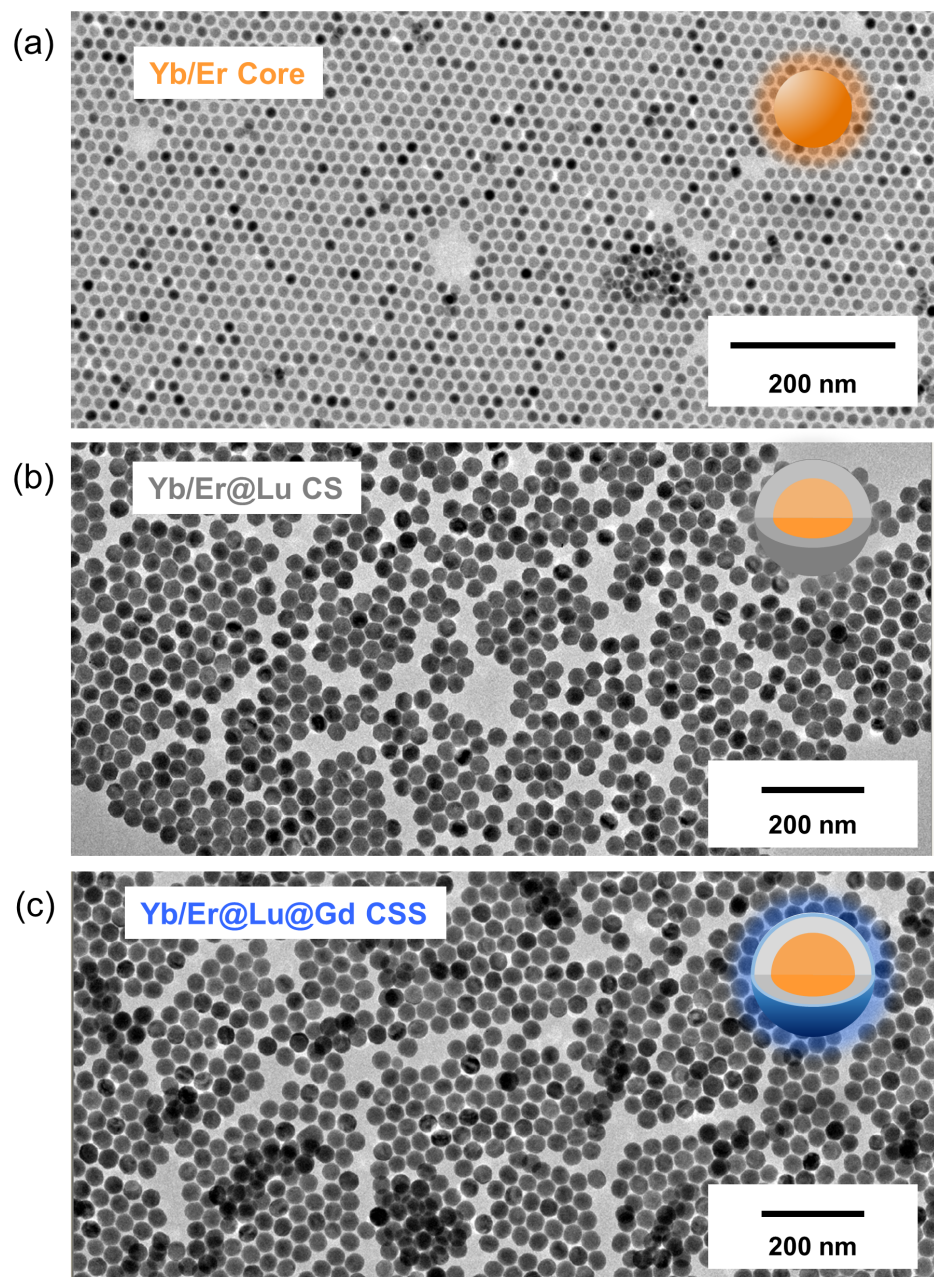


Figure S4 Low magnification TEM images of the core, CS and CSS NPs.

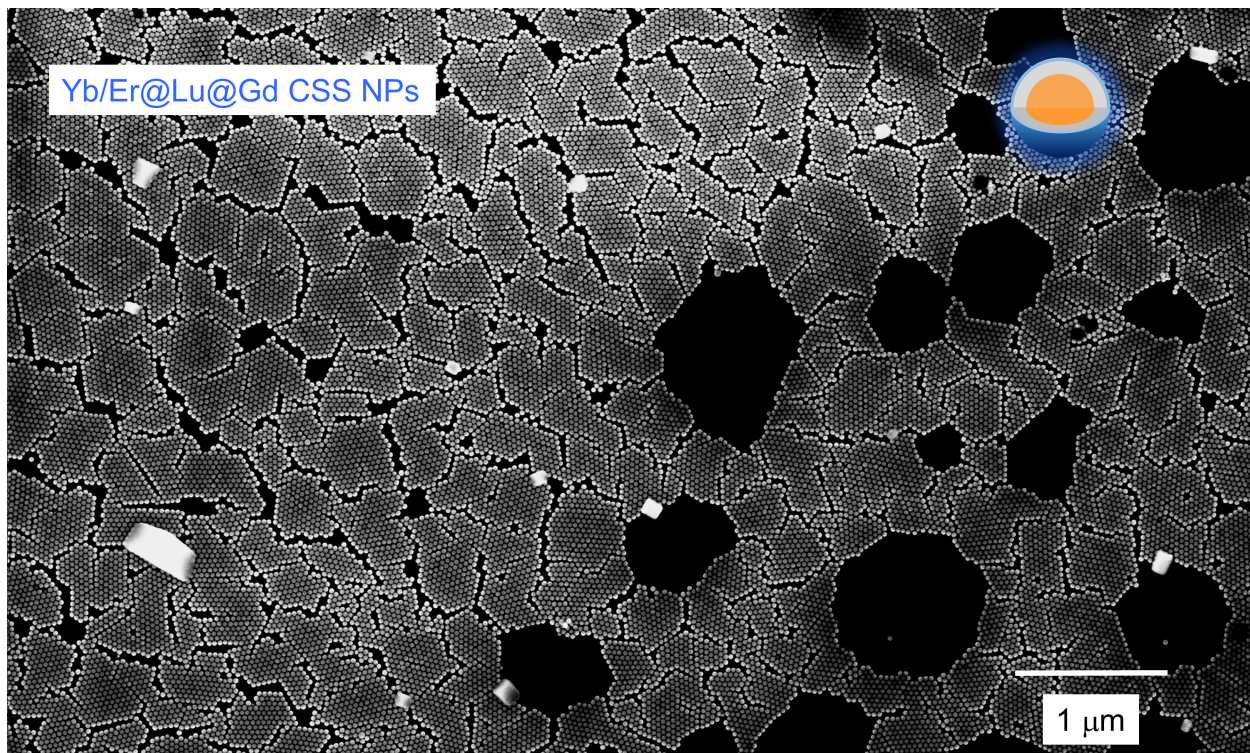


Figure S5 Low magnification SEM image of the β -NaYb/ErF₄@NaLuF₄@NaGdF₄ CSS NPs showing their excellent uniformity and monodispersity.

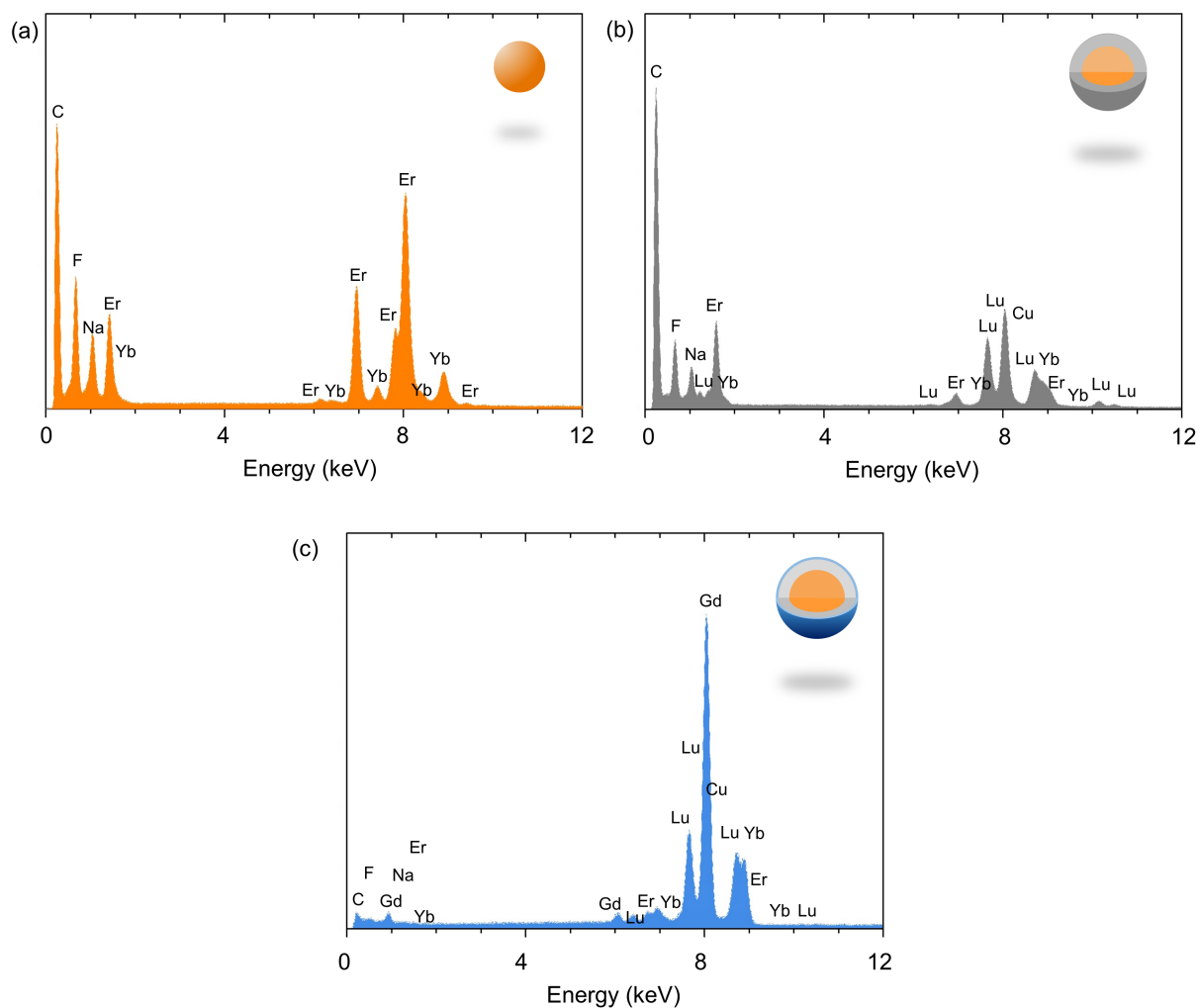


Figure S6 Energy dispersive X-ray spectroscopy (EDS) of (a) β -NaYb/ErF₄ core, (b) β -NaYb/ErF₄@NaLuF₄ CS, and (c) β -NaYb/ErF₄@NaLuF₄@NaGdF₄ CSS NPs showing the elemental composition of each structure. The peak of carbon and copper comes from the sample grid of TEM.

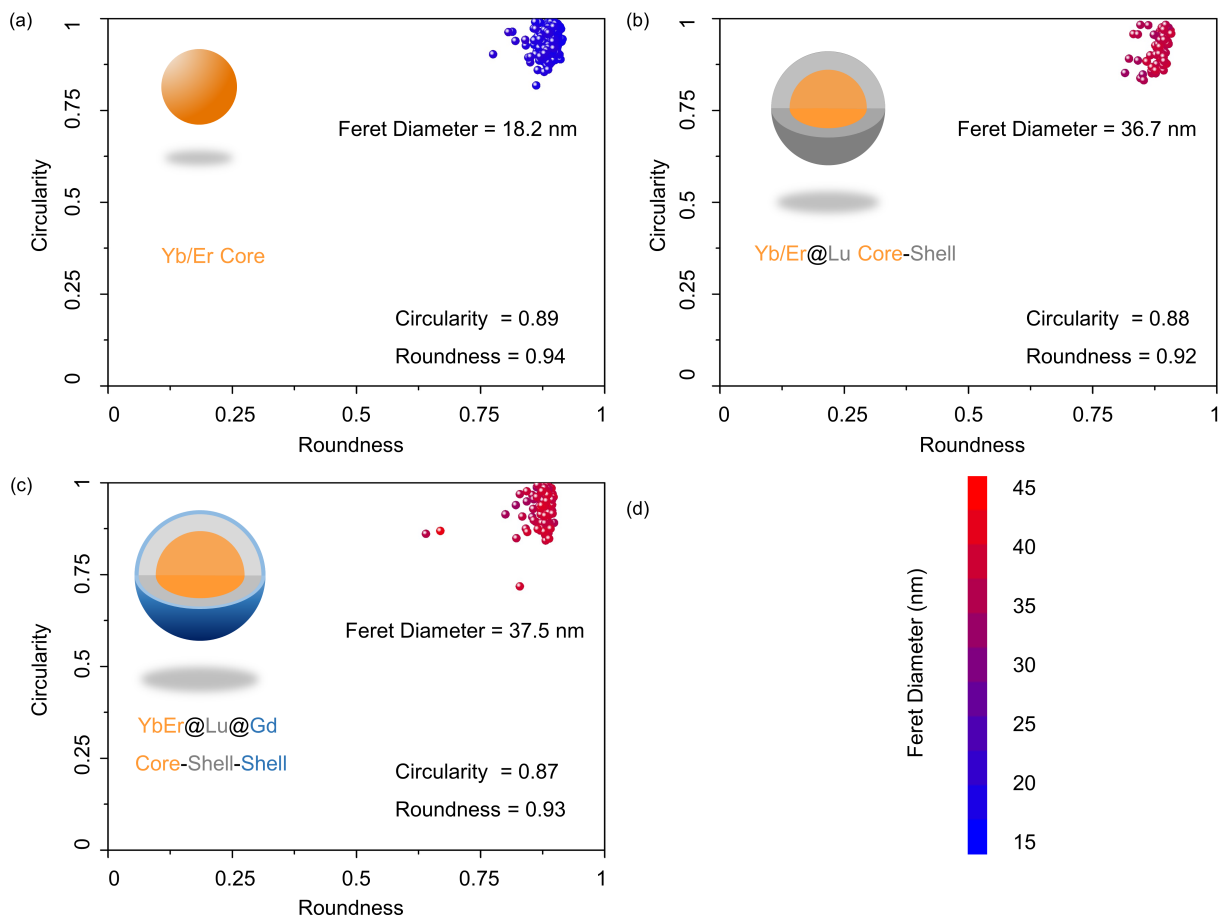


Figure S7 Morphological characterization of the (a) core, (b) CS, and (c) CSS NPs shown in Figure 1.

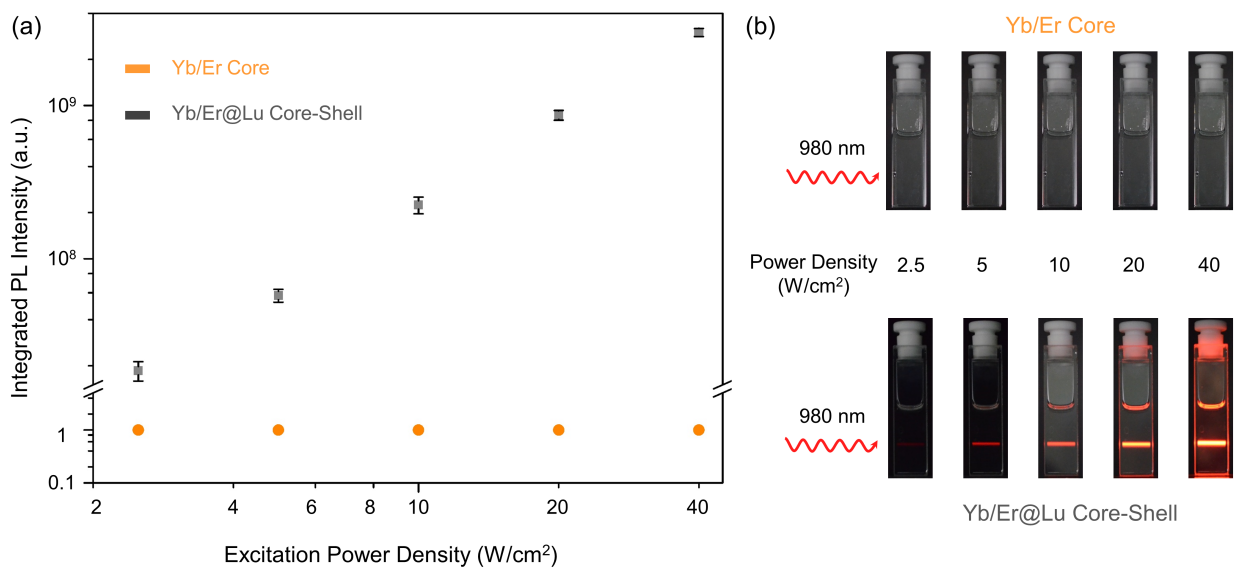


Figure S8 (a) Power density-dependent PL intensity of Yb/Er core and Yb/Er@Lu CS NPs. There is no emission peaks for the Yb/Er cores and we denoted the emission intensity as 1. (b) Photographs of samples excited at 980 nm with variable laser power density.

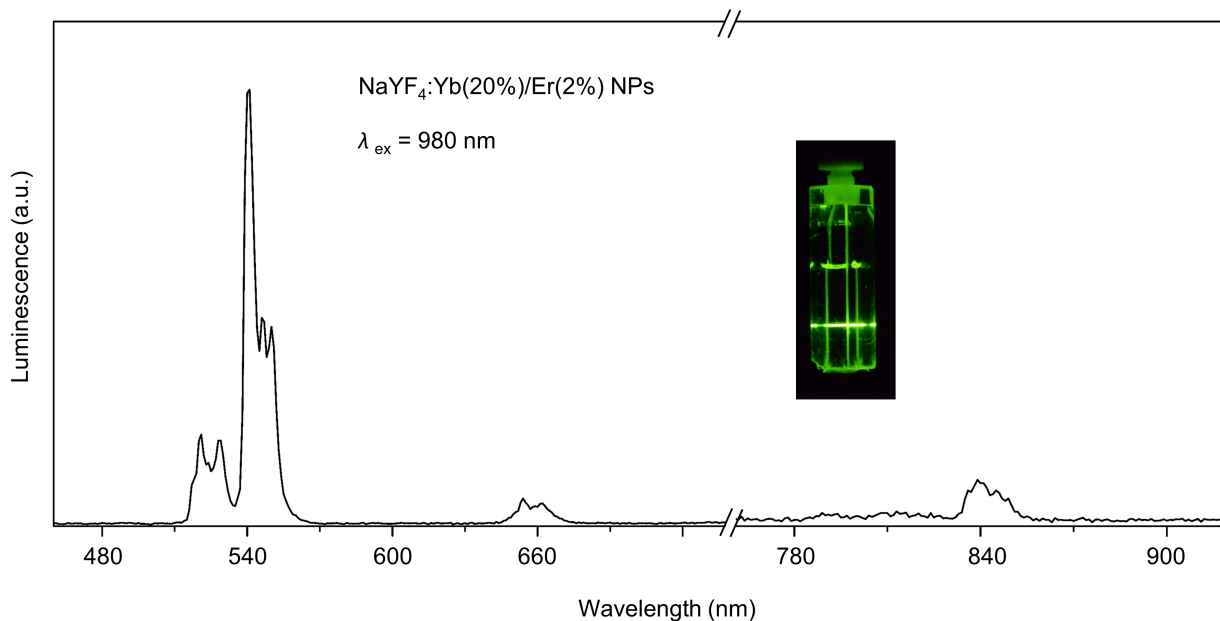


Figure S9 PL spectra of NaYF₄:Yb(20%)/Er(2%) NPs excited at 980 nm, showing major emission in the visible green regime instead of visible red and NIR regime.

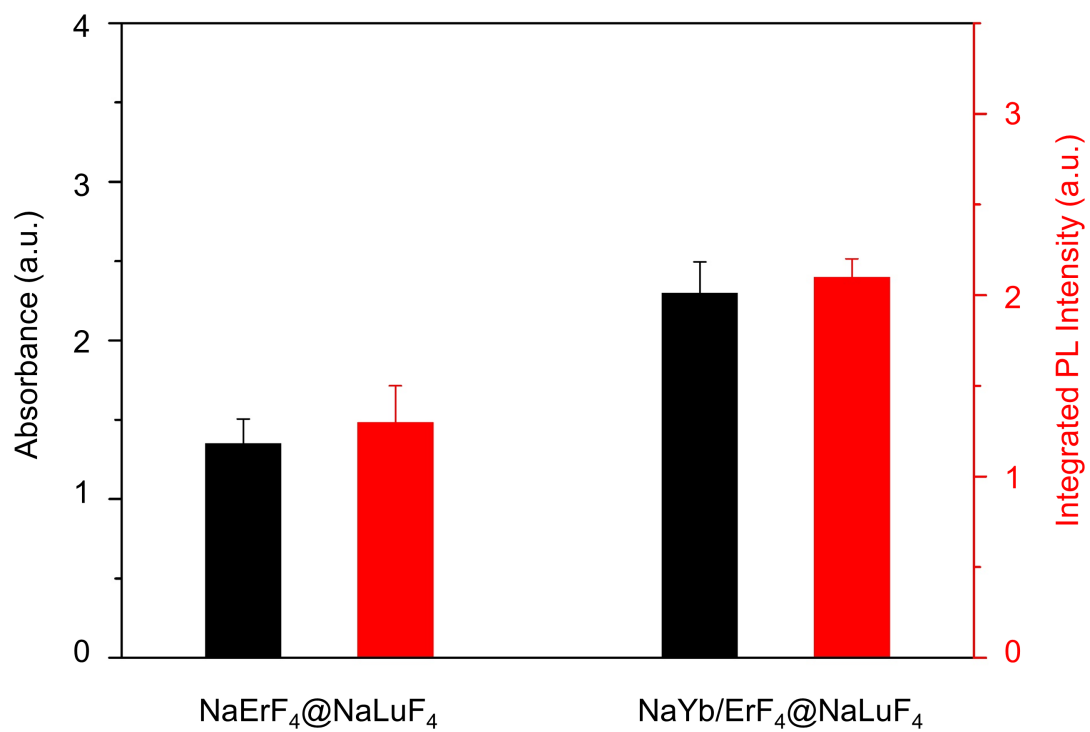


Figure S10 Absorbance at 980 nm and integrated PL intensity of Er@Lu CS NPs and Yb/Er@Lu CS NPs.

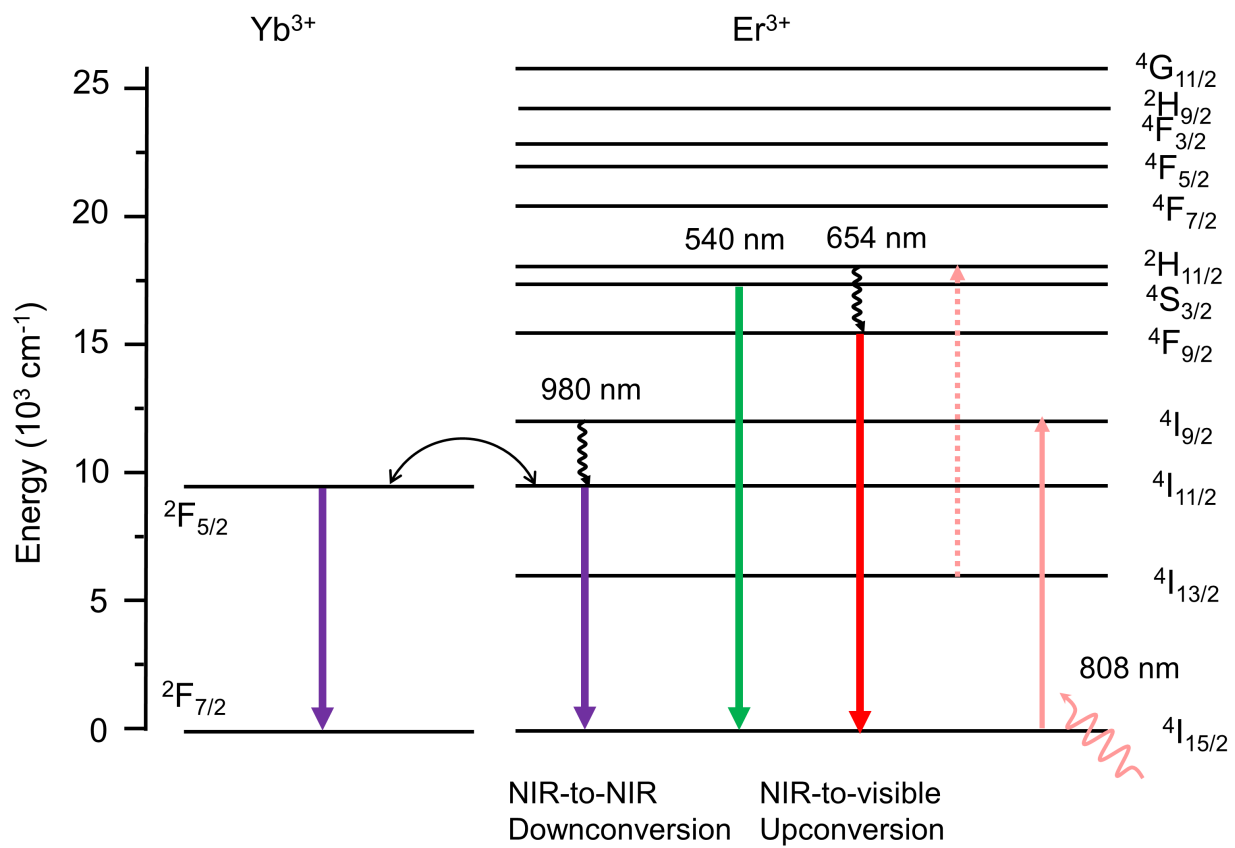


Figure S11 Simplified energy level diagram of Yb³⁺/Er³⁺ luminescent pair showing excitation at 808 nm.

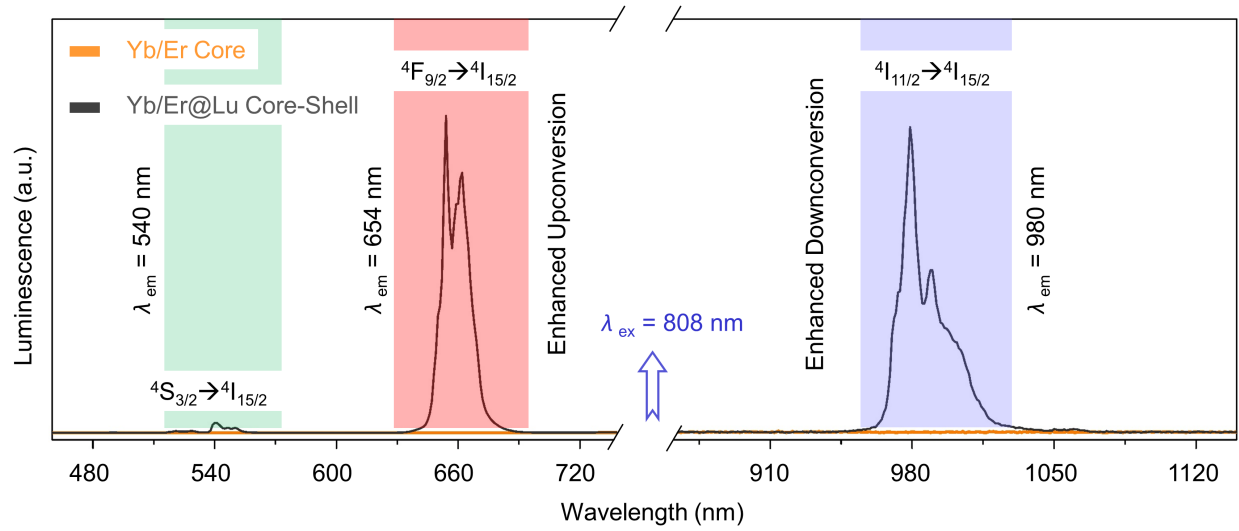


Figure S12 PL spectra across the visible and NIR regime of the Yb/Er core NPs and Yb/Er@Lu CS NPs with 808 nm excitation.

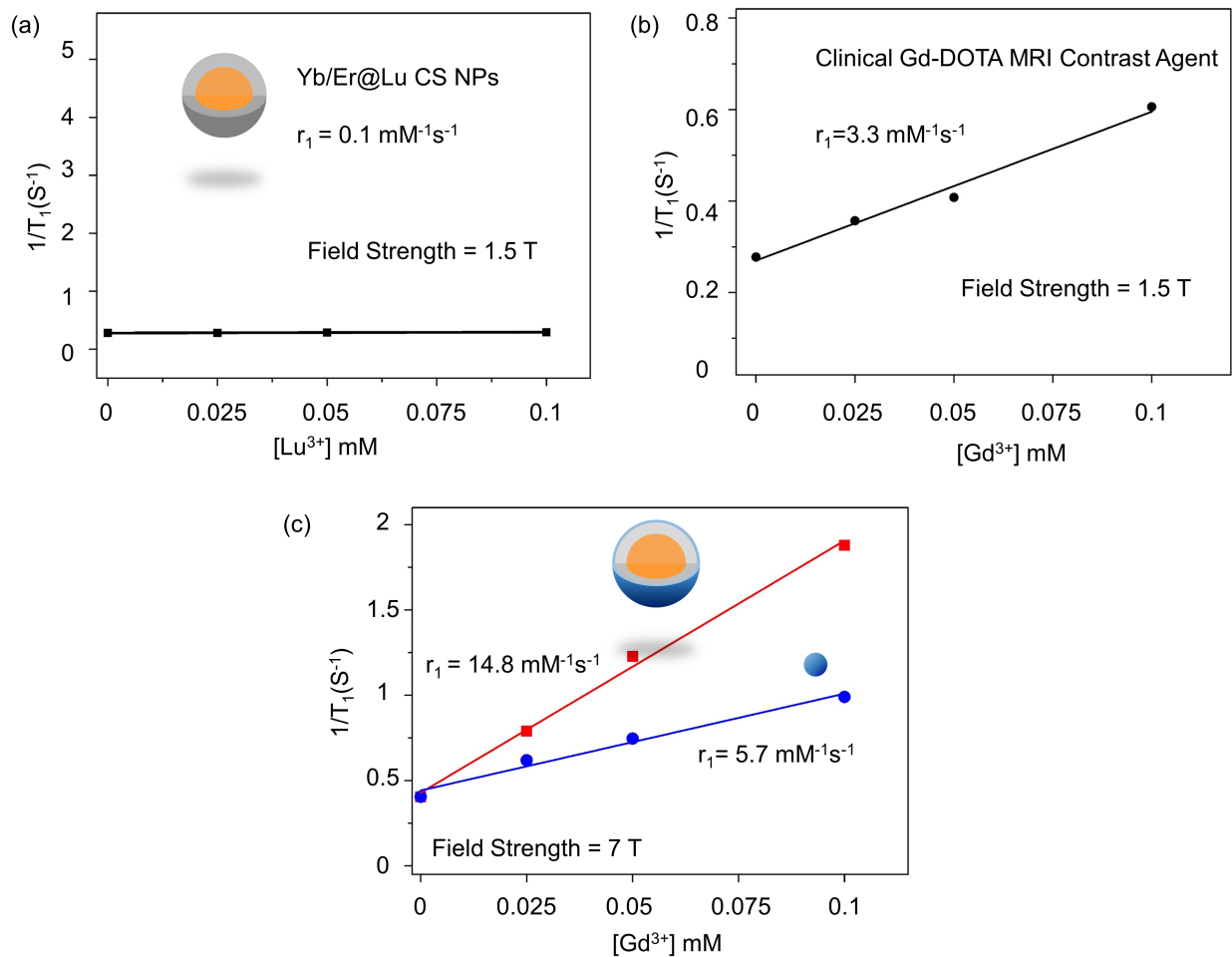


Figure S13 (a) r_1 relaxivity of the Yb/Er@Lu CS NPs at the magnetic field strength of 1.5T. (b) r_1 relaxivity of the clinical Gd-DOTA MRI contrast agents at the magnetic field strength of 1.5 T. (c) r_1 relaxivity of the CSS NPs and α -NaGdF₄ NPs at the magnetic field strength of 7.0 T.

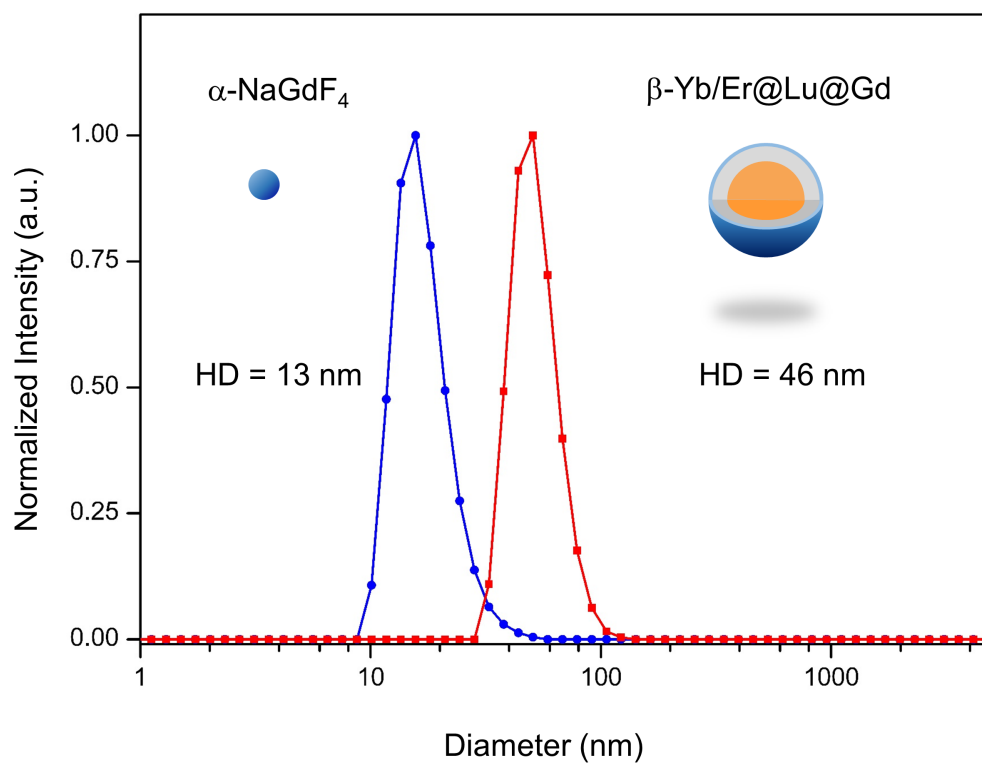


Figure S14 Hydrodynamic diameters (HD) of the α -NaGdF₄ and β -Yb/Er@Lu@Gd CSS NPs.

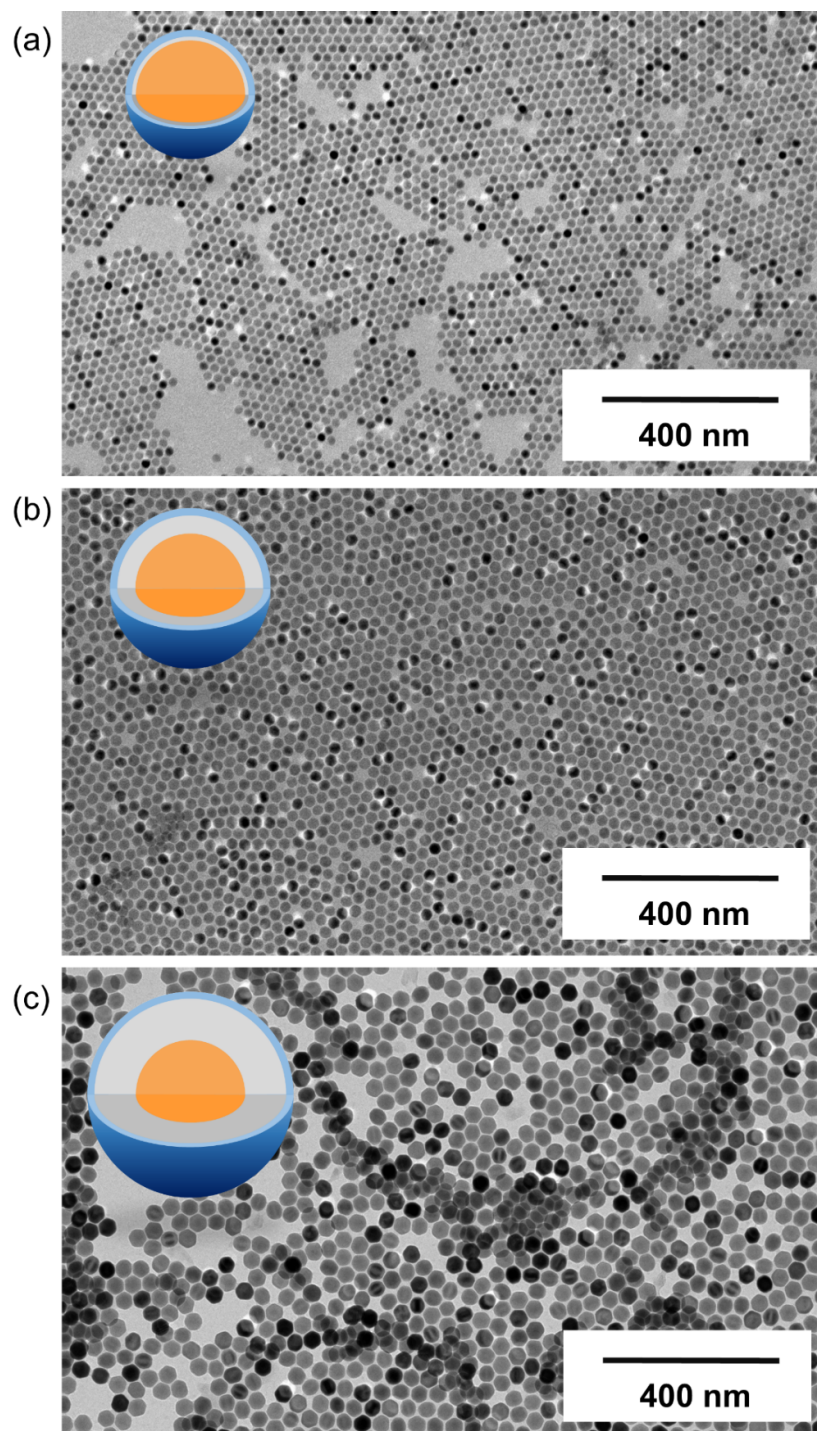


Figure S15 Low magnification TEM images of the (a) core, (b) CS, (c) CSS NPs with tunable thickness of the interfacial NaLuF_4 layer.

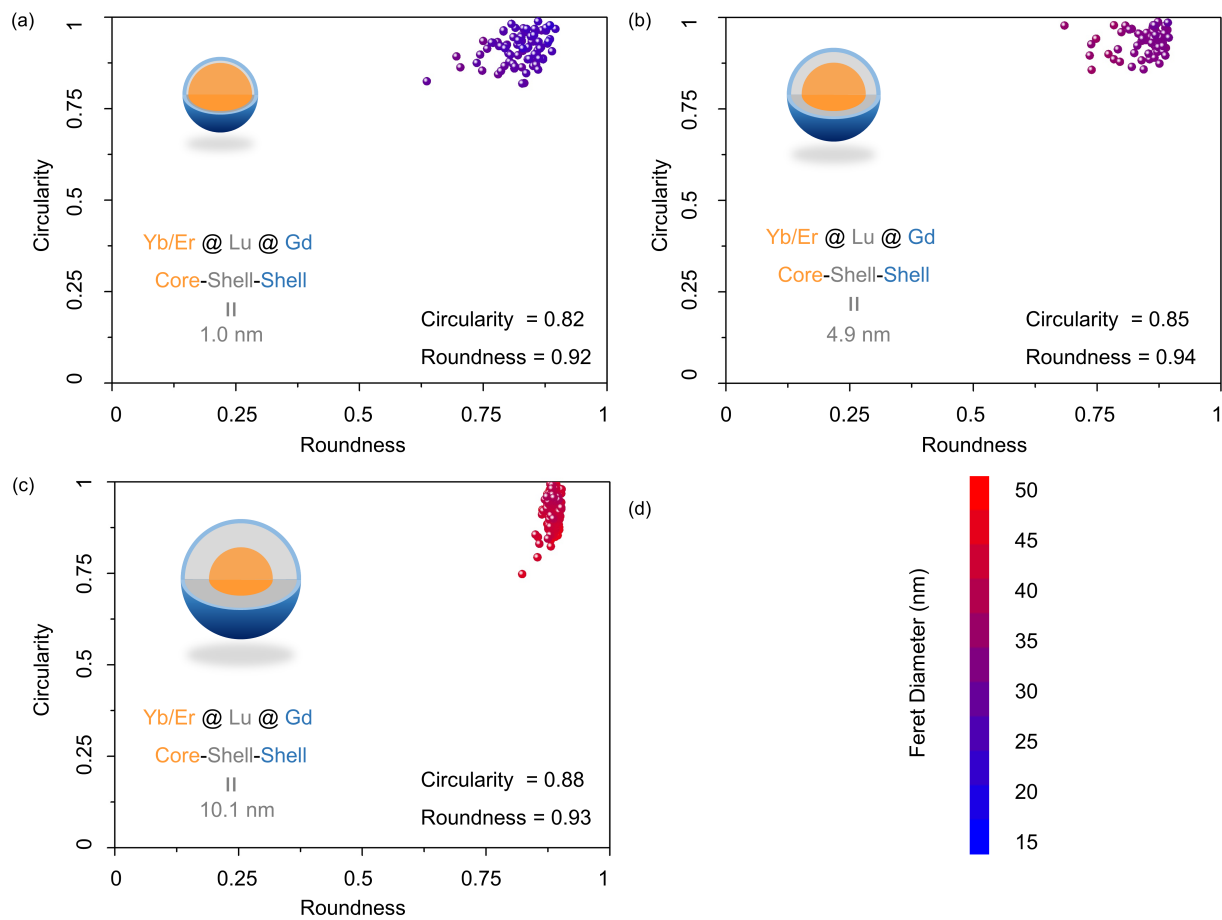


Figure S16 Morphological characterization of the (a) core, (b) CS, and (c) CSS NPs with increased interfacial NaLuF₄ layer thickness.

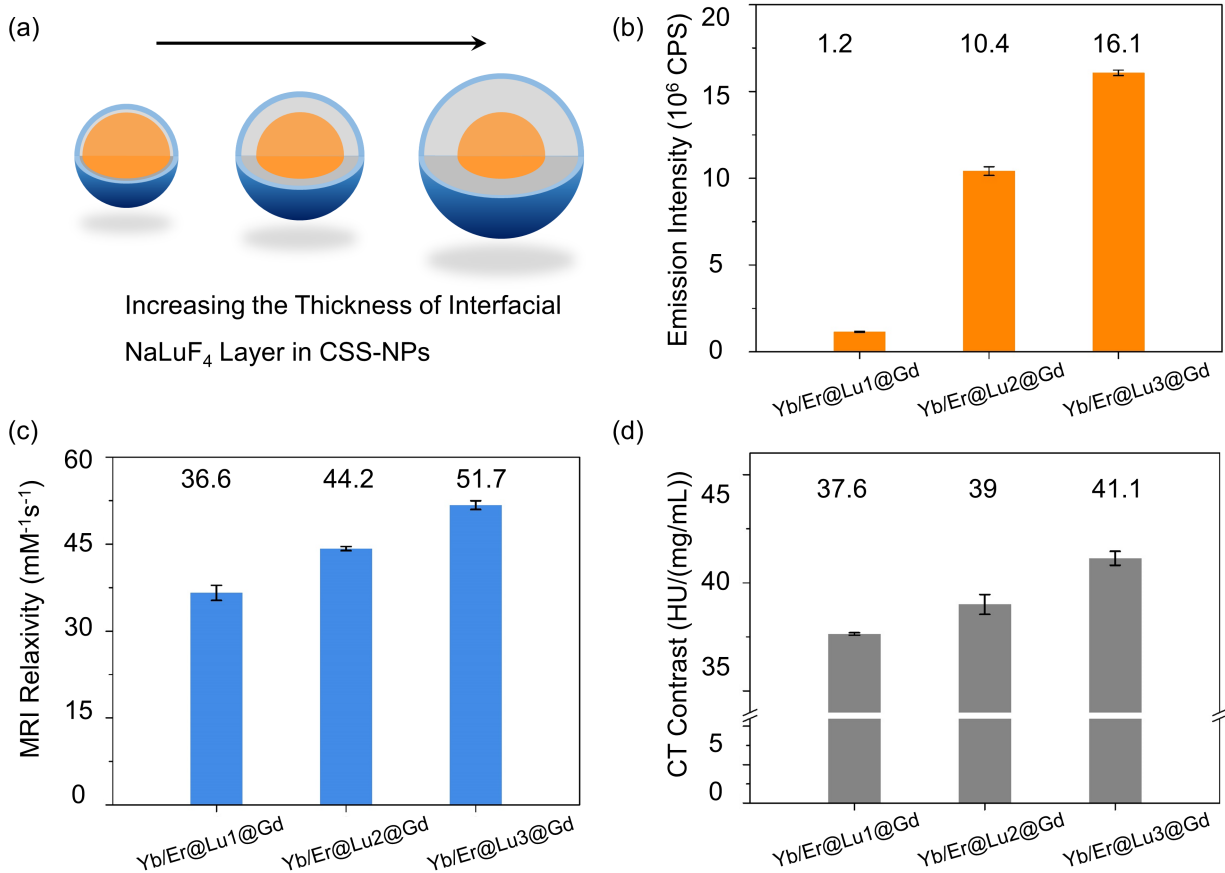


Figure S17 Comparison of PL emission intensity, MRI relaxivity, and CT contrast with increasing thickness of the interfacial NaLuF₄ layer.

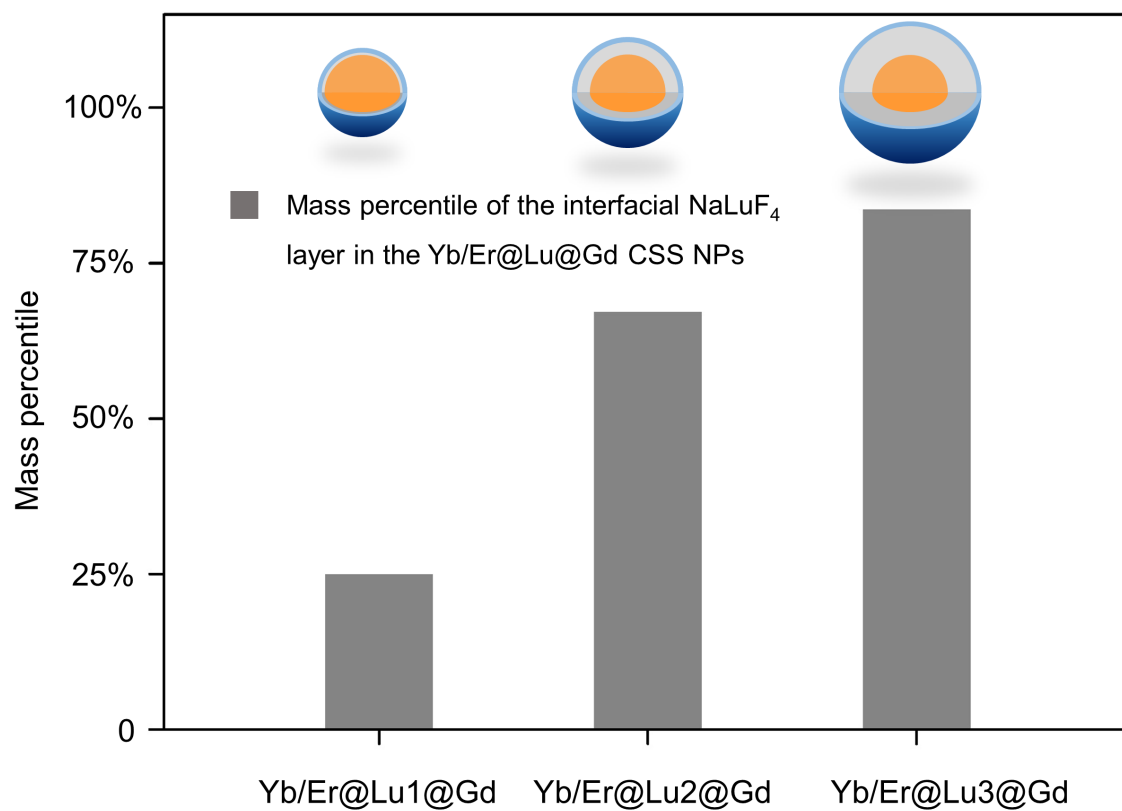


Figure S18 Mass percentile change of the interfacial NaLuF₄ layer in the Yb/Er@Lu@Gd CSS NPs with increased amount of sacrificial α - NaLuF₄ NPs deposited on the Yb/Er core NPs.

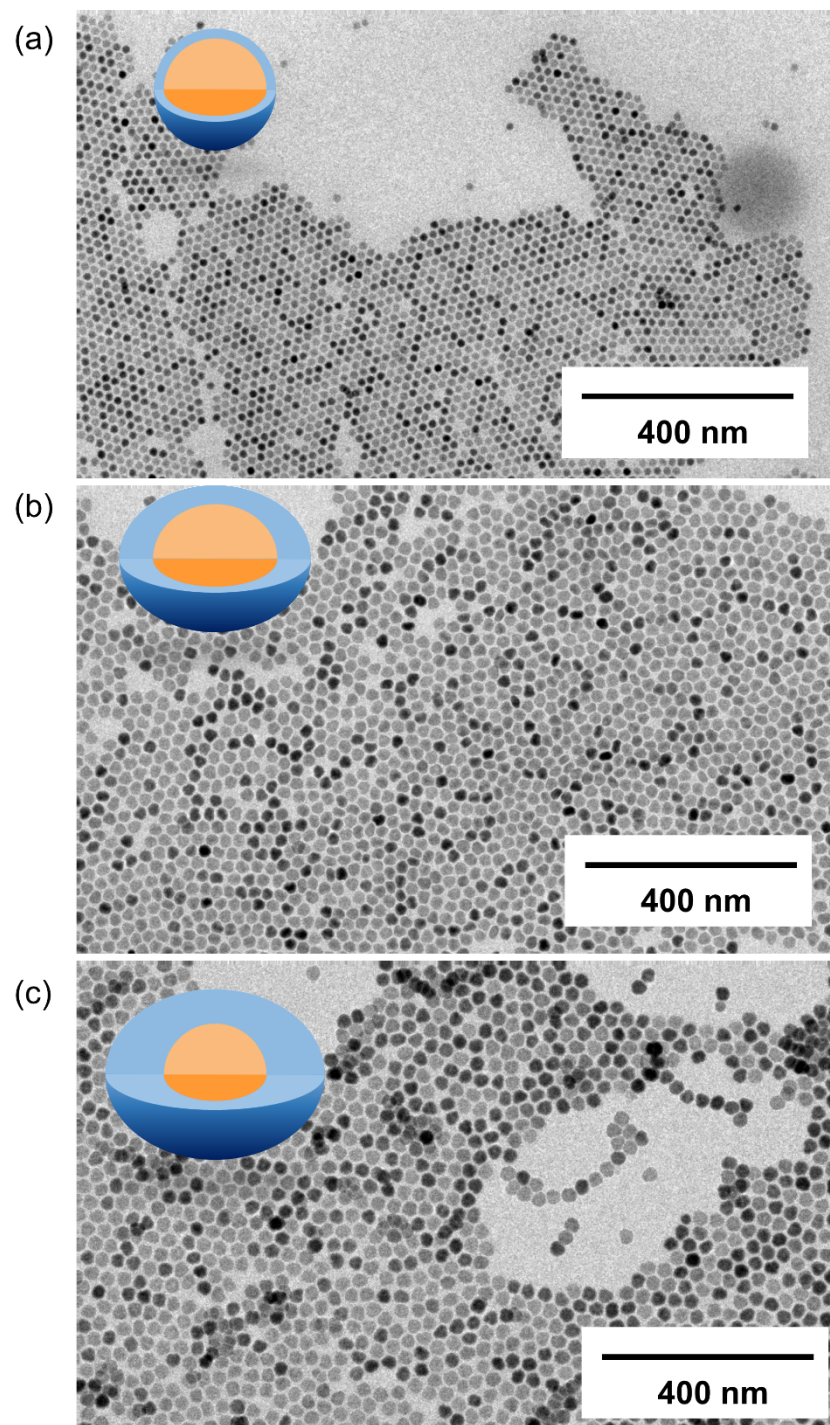


Figure S19 Low magnification TEM images of the Yb/Er@Gd1, Yb/Er@Gd2 and Yb/Er@Gd3 CS-NPs with increasing NaGdF₄ shell thickness.

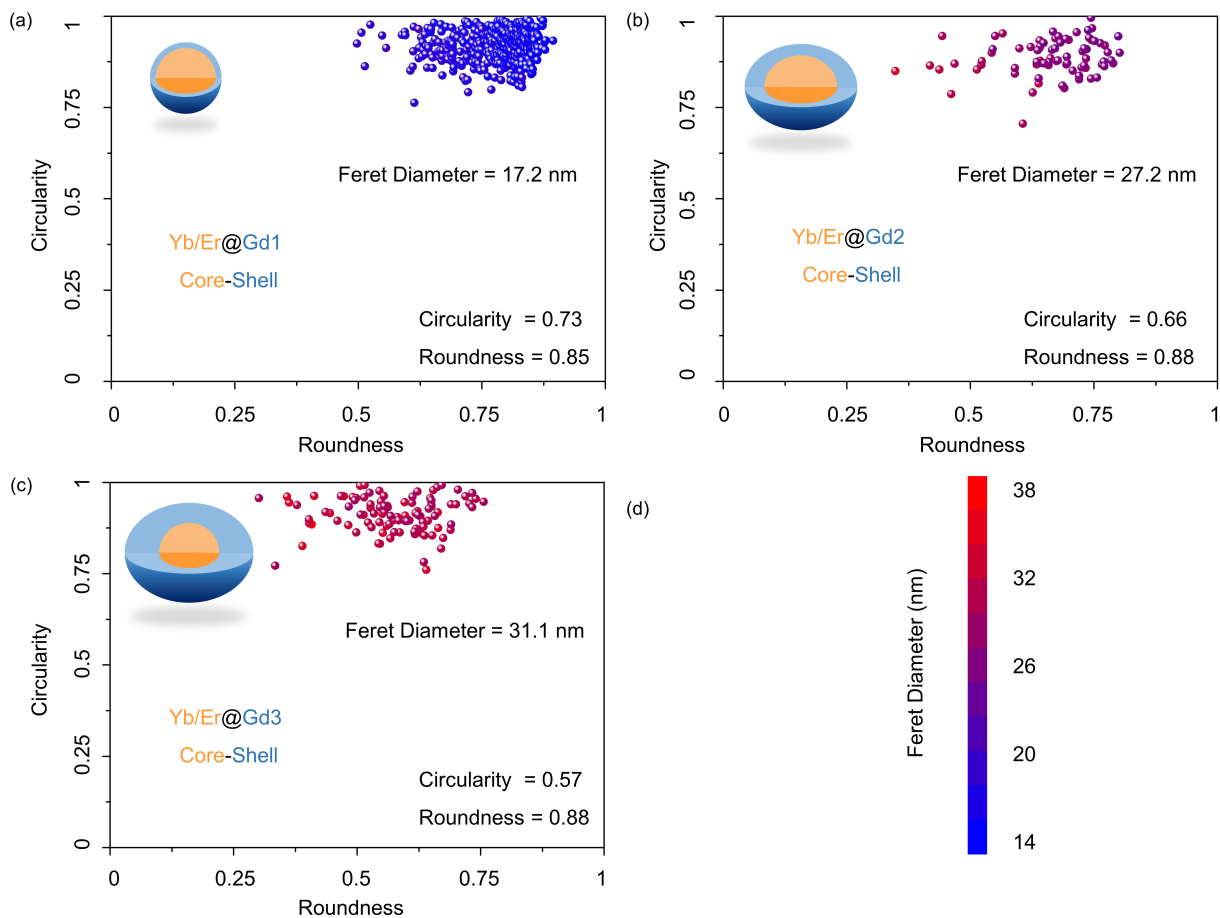


Figure S20 Morphological characterization of the (a) core, (b) CS and (c) CSS NPs shown in Figure 6.

REFERNCES:

1. Johnson, N. J. J.; He, S.; Diao, S.; Chan, E. M.; Dai, H. J.; Almutairi, A. *J. Am. Chem. Soc.* **2017**, *139*, 3275-3282.
2. Bronstein, N. D.; Yao, Y.; Xu, L.; O'Brien, E.; Powers, A. S.; Ferry, V. E.; Alivisatos, A. P.; Nuzzo, R. G. *ACS Photonics* **2015**, *2*, 1576-1583.
3. Johnson, N. J. J.; He, S.; Hun, V. A. N.; Almutairi, A. *ACS Nano* **2016**, *10*, 8299-8307.
4. Tong, S.; Hou, S.; Ren, B.; Zheng, Z.; Bao, G. *Nano Lett.* **2011**, *11*, 3720-3726.
5. Johnson, N. J. J.; van Veggel, F. *ACS Nano* **2014**, *8*, 10517-10527.
6. Shannon, R. D. *Acta Crystallogr. Sect. A* **1976**, *32*, 751-767.
7. Viswanathan, S.; Kovacs, Z.; Green, K. N.; Ratnakar, S. J.; Sherry, A. D. *Chem. Rev.* **2010**, *110*, 2960-3018.